

## Rapid dendritic growth of Al-Ge hypoeutectic alloy in a drop tube\*

LIU Xiangrong\*\*, CAO Chongde and WEI Bingbo

(Department of Applied Physics, Northwestern Polytechnical University, Xi'an 710072, China)

Received August 29, 2002

**Abstract** Dendritic growth in Al-45% Ge hypoeutectic alloy has been investigated during free fall in a 3 m drop tube. Calculations indicate that the undercooling obtained for the falling Al-45% Ge droplets ranges from 13 K to 201 K. The maximum undercooling attains  $0.27T_L$ . With the increase of undercooling, the primary (Al) phase undergoes a "columnar dendrite to equiaxed dendrite" structural transition. According to the current rapid dendritic growth theory, the growth of primary (Al) phase is always controlled by solute diffusion.

**Keywords:** dendritic growth, undercooling, containerless processing, Al-Ge alloy.

Dendrite is the most popular morphology in the solidification of materials. Rapid dendritic growth in undercooled liquid melt is an important subject in the field of materials physics<sup>[1-3]</sup>. In the recent decades, some theoretical models have been set up to describe the dendritic growth<sup>[4-6]</sup>. The Lipton-Kurz-Trivedi/Bottinger-Coriell-Trivedi (LKT/BCT) model is the most successful theory for rapid dendritic growth<sup>[7]</sup>. However, it is necessary to investigate the morphology transition characteristics and the corresponding mechanism of rapid dendritic growth.

Containerless processing technique is an efficient method to achieve high undercooling in liquid alloy melts, including various levitation techniques and drop tube technique, etc.<sup>[8]</sup> In particular, drop tube is unique to combine containerless state, microgravity with rapid cooling. It is expected to achieve large undercooling and rapid crystal growth in drop tube processing<sup>[9,10]</sup>.

The object of this work is to study the thermal history, the microstructure transition and the dendritic growth kinetics of Al-45% Ge hypoeutectic alloy.

### 1 Experimental procedure

The master alloy with a mass of about 0.5 g was prepared from pure Al (99.99%) and pure Ge

(99.999%) in an arc-melting furnace under argon atmosphere. The sample was placed in a  $\Phi 16$  mm  $\times$  150 mm quartz tube with a  $\Phi 0.3$  mm orifice at its bottom. The quartz tube was then installed at the top of a 3 m drop tube. After being evacuated to  $2.0 \times 10^{-5}$  Pa, the drop tube was backfilled with a mixture of He and Ar to 1 atm<sup>1)</sup>. The sample was inductively melted and overheated by 200 K, and then, the melt was ejected through the orifice and dispersed into many fine droplets by exerting a high pressure gas flow of Ar into the quartz tube. The temperature was monitored by an NQO6/11C3.4V250 infrared pyrometer during melting.

The solidified droplets were sieved into several groups according to their sizes. Then, they were mounted, sectioned, polished, and etched with 10% NaOH alcohol solution. The microstructures were analyzed by an S2700 scanning electron microscope.

### 2 Results and discussions

The phase diagram of the Al-Ge binary eutectic alloy system is shown in Fig. 1. The equilibrium eutectic composition is Al-51.6wt% Ge. The eutectic transition  $L \rightarrow (Al) + (Ge)$  occurs at 693.16 K for the composition range of 5.2~99.6% Ge. The location of Al-45% Ge hypoeutectic alloy and the maximum undercooling achieved in the experiments are given in Fig. 1.

\* Supported by the National Natural Science Foundation of China (Grant Nos. 50221101 and 50201013)

\*\* To whom correspondence should be addressed. E-mail: lms@nwpu.edu.cn

1) 1 atm = 101325 Pa

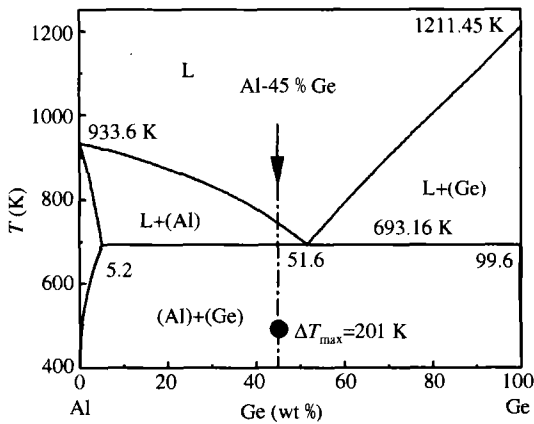


Fig. 1. Phase diagram of the Al-Ge binary system.

2.1 Morphological transition of primary (Al) phase

The size of droplets obtained in the drop tube ranges from 100 μm to 1000 μm in diameter, whose microstructures are shown in Fig.2. Droplets larger

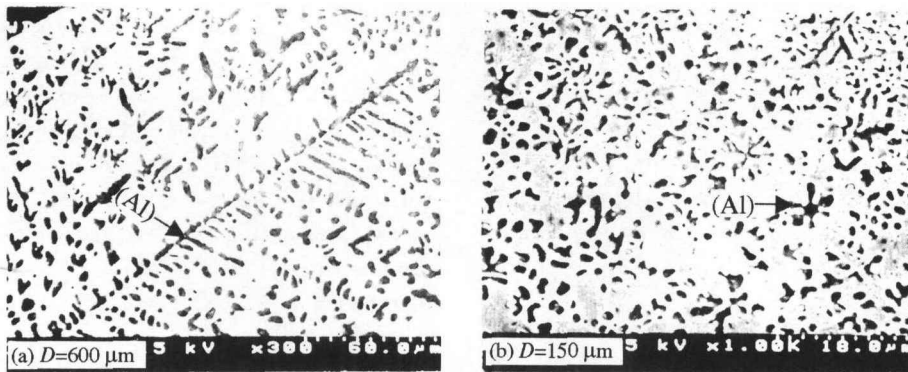


Fig. 2. Microstructures of Al-45% Ge droplets with different sizes.

2.2 Calculations of undercooling and cooling rate

During free fall of the small droplets with diameters of micrometer order, it is difficult to measure and record their temperature. Fortunately, the thermal history of the small droplets<sup>[11]</sup> can be calculated by combining the Newtonian heat transfer model<sup>[12,13]</sup> and the classical nucleation theory<sup>[14,15]</sup>. In this model, the droplet is assumed to keep the spherical shape during free fall and the heat is mainly transferred by radiation and convection, neglecting thermal convection inside the droplet. The relationship between nucleation temperature  $T_N$  and droplet diameter  $D$  is described by two functions  $\Phi$  and  $\Psi$ :

$$\frac{\Psi(T_N, D)}{T_N \cdot \Delta T^2} = \ln \Phi(T_N, D) \quad (1)$$

$$\Phi(T_N, D) =$$

than 550 μm in diameter show coarse columnar dendrites distributed in the eutectic matrix and the maximum length of dendrites attains 240 μm, as presented in Fig. 2 (a). With the reduction of droplet diameter, primary (Al) dendrites are refined. When the droplet diameter ( $D$ ) is smaller than 200 μm, the microstructure is characterized by equiaxed primary (Al) dendrites dispersed in the eutectic matrix, as illustrated in Fig. 2 (b). Apparently, with the decrease in droplet size, a “columnar dendrite to equiaxed dendrite” morphological transition occurs to primary (Al) phase. This is due to the increase in undercooling and cooling rate with the decrease in droplet size. High undercooling tends to increase nucleation rate and enhance dendrite fragmentation during intense recalescence. Meanwhile, rapid cooling weakens the coarsening of primary (Al) dendrites during processing in the drop tube.

$$\frac{\frac{\pi}{6} D^3 K_V \Delta T^3 T_N^2}{\Psi(T_N, D) \left( -\frac{dT_d}{dt} \right) (3T_L - T_N) + [\kappa + 2\epsilon(T_N - T_g)] \Delta T^3 T_N^2} \quad (2)$$

Here,

$$\Psi(T_N, D) = \frac{16\pi\sigma_{SL}^3 T_L^2 f(D)}{3k_B \rho_d^2 \Delta H^2}, \quad (3)$$

$$\kappa = \frac{12k_g}{\rho_d C_P D^2}, \quad (4)$$

where  $\Delta T$  is the undercooling attained before nucleation,  $K_V$  the nucleation kinetic parameter ( $10^{40} \text{ m}^{-3} \text{ s}^{-1}$ ),  $T_D$  the temperature of droplet,  $T_L$  the liquidus temperature,  $T_g$  the gas temperature in drop tube,  $\epsilon$  the thermal radiation coefficient,  $k_B$  the Boltzmann constant,  $k_g$  the thermal convection coefficient of gas,  $\sigma_{SL}$  the liquid-solid interfacial energy,  $\rho_D$  the density of droplet,  $C_P$  the specific heat of liquid,  $\Delta H$  the heat of fusion. Parameters used in calcu-

lations are listed in Table 1.

On the basis of Eqs. (1)~(4), the relationships of functions  $\Psi(T_N, D)/T_N\Delta T^2$  and  $\ln \Phi(T_N, D)$  to nucleation temperature  $T_N$  are calculated, as shown in Fig. 3. The nucleation temperatures of the droplets with various sizes can be determined from the intersections. Furthermore, the corresponding undercoolings are available. The undercooling as a function of droplet size is given in Fig. 4. It is obvious that the undercooling is enhanced when droplet size decreases. For droplets of 1000~100  $\mu\text{m}$  in diameter, the undercooling covers a range of 13~201 K, and the maximum undercooling attains 0.27  $T_L$ .

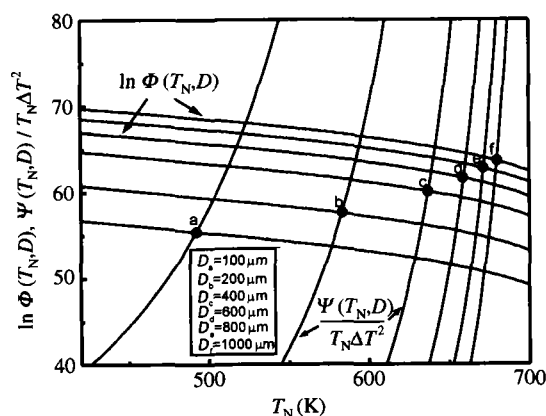


Fig. 3. Function  $\ln \Phi(T_N, D)$  and  $\Psi(T_N, D)/T_N\Delta T^2$  versus nucleation temperature.

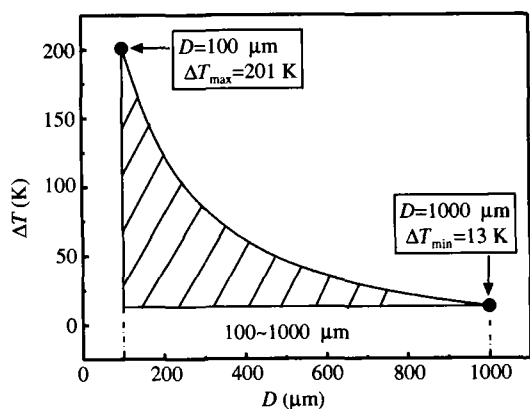


Fig. 4. Undercooling as a function of droplet diameter.

### 2.3 Kinetics of rapid dendrite growth

So far, the LKT/BCT dendritic growth theory has been proven to be the most successful model for describing the kinetics of rapid dendritic growth<sup>[4-6]</sup>. In order to reveal the growth mechanism of primary (Al) phase in the Al-45% Ge alloy, the interrelationships of the dendritic growth velocity

$V$ , the dendrite tip radius  $R$ , the partial undercooling  $\Delta T_P$  (including thermal undercooling  $\Delta T_t$ , solutal undercooling  $\Delta T_c$ , curvature undercooling  $\Delta T_r$  and kinetic undercooling  $\Delta T_k$ ) with the bulk undercooling  $\Delta T$  are calculated respectively on the basis of this model. The results are shown in Figs. 5 and 6, respectively. From Fig. 5, it can be seen that with the increase of undercooling, the dendritic growth velocity increases whereas the dendrite tip radius decreases. The dendritic growth velocity and the dendrite tip radius are 21 mm/s and 0.032  $\mu\text{m}$  respectively at the maximum undercooling 201 K. Fig. 6 demonstrates that the solutal undercooling always plays a main role, indicating that the growth of primary (Al) phase is constantly controlled by solute diffusion.

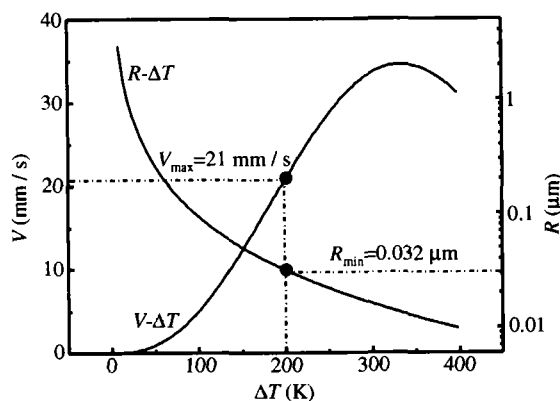


Fig. 5. Dendritic growth velocity and dendrite tip radius versus undercooling.

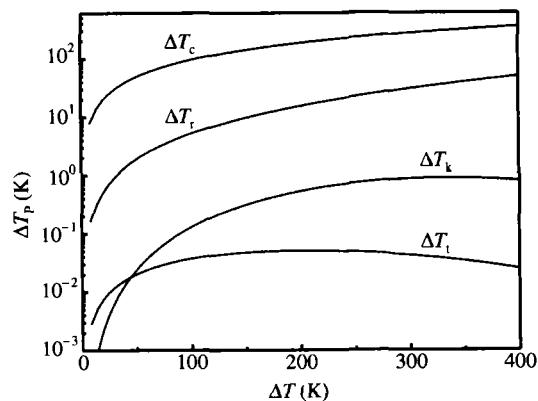


Fig. 6. Partial undercooling  $\Delta T_P$  as a function of bulk undercooling  $\Delta T$ .

Table 1. The thermophysical parameters used in calculations<sup>[16,17]</sup>

Parameter	Value
Eutectic equilibrium temperature (K)	693.16
Superheating (K)	200

To be continued

Continued

Parameter	Value
Thermal radiation coefficient	0.22
Specific heat of the melt ( $J \cdot mol^{-1} K^{-1}$ )	30.82
Heat of fusion ( $J \cdot mol^{-1}$ )	16588
Length of the eutectic line (wt% Ge)	94.4
Solute diffusion coefficient ( $m^2 \cdot s^{-1}$ )	$2.19 \times 10^{-7} \exp(-36332/RT)$
Liquid-solid interface energy ( $J \cdot m^{-2}$ )	0.31
Gibbs-Thomson coefficient for (Al) ( $K \cdot m$ )	$2.43 \times 10^{-7}$
Capillarity constant of (Ge) phase ( $m \cdot wt\%$ )	$2.41 \times 10^{-7}$
Equilibrium partition coefficient of (Al) phase	0.1
Equilibrium partition coefficient of (Ge) phase	0.008
Gas density in drop tube ( $kg \cdot m^{-3}$ )	1.249
Gas viscosity in drop tube ( $Pa \cdot s$ )	44.77
Thermal conductivity ( $W \cdot m^{-1} K^{-1}$ )	126.3
Gas temperature (K)	298

### 3 Conclusions

(1) Al-45% Ge hypoeutectic alloy is rapidly solidified during containerless processing in a drop tube. The calculated undercooling of the droplets ranges from 13 K to 201 K, and the maximum undercooling attains  $0.27 T_L$ .

(2) With the increase of undercooling, a "columnar dendrite to equiaxed" structural transition occurs to primary (Al) phase.

(3) The calculated growth velocity of primary (Al) phase in Al-45% Ge alloy is 21 mm/s at the maximum undercooling. The growth of primary (Al) phase is always controlled by solute diffusion.

**Acknowledgement** The authors would like to thank Dr. Wang Nan, Dr. Han Xiujun, Dr. Xie Wenjun and Dr. Yao Wenjing for their help during experiments.

### References

- Eckler, K. et al. Grain refinement in solidification of undercooled Ni-Cu melts. *Mater. Sci. Forum.*, 1996, 215~216; 45.
- Lu, X. Y. et al. Phase selection and microstructure evolution of undercooled Fe92Cu8 peritectic alloy. *Progress in Natural Science*, 1999, 9: 286.
- Han, X. J. et al. Phase separation and microstructural characteristics of undercooled Cu-Pb immiscible alloy. *Progress in Natural Science*, 2001, 11: 602.
- Lipton, J. et al. Rapid dendrite growth in undercooled alloys. *Acta Metall.*, 1987, 35: 957.
- Trivedi, R. et al. Effect of growth rate dependent partition coefficient on the dendritic growth in undercooled melts. *Acta Metall.*, 1987, 35: 965.
- Boettinger, W. J. et al. Solute redistribution during rapid solidification. In: *Proc. 4th Conf. on Rapid Solidification Processing: Principles and Technologies IV*, Claitors: Baton Rouge, 1987, 13.
- Leonhardt, M. et al. Metastable phase formation in undercooled eutectic NiSi melts. *Mater. Sci. Eng.*, 1999, A271: 31.
- Herlach, D. M. et al. Containerless processing in the study of metallic melts and their solidification. *Int. Mater. Rev.*, 1993, 38: 273.
- Fransaer, J. et al. Solidification of Ga-Mg-Zn in a gas-filled drop tube: experiments and modelling. *J. Appl. Phys.*, 2000, 87: 1801.
- Cao, C. D. et al. Peritectic solidification of highly undercooled Co-Cu alloy. *Adv. Space Res.*, 1999, 24: 1251.
- Lee, E. S. et al. Solidification progress and heat transfer analysis of gas-atomized alloy droplets during spray forming. *Acta Metall. Mater.*, 1994, 42: 3231.
- Levi, C. G. et al. Heat flow during rapid solidification of undercooled metal droplets. *Metall. Trans. A*, 1982, 13A: 221.
- Welty, J. R. et al. *Fundamentals of Momentum, Heat and Mass Transfer*. 3rd ed. New York: Wiley, 1984, 326.
- Cantor, B. et al. Heterogeneous nucleation in solidifying alloys. *Acta Metall.*, 1979, 27: 33.
- Libera, M. et al. Heterogeneous nucleation of solidification in atomized liquid metal droplets. *Mater. Sci. Eng. A*, 1991, 132: 107.
- Iida, T. et al. *The Physical Properties of Liquid Metals*. Oxford: Clarendon Press, 1993.
- Brandes, E. A. *Smithells Metals Reference Book*, 6th ed. England: Butterworth, 1983.